Electronic Supplementary Material (ESI) for Nanoscale.
This journal is © The Royal Society of Chemistry 2018

Supporting Information

Scalable synthesis of foam-like FeS_2 nanostructure by a solution combustion-sulfurization process for high-capacity sodium-ion battery

Rudan Hu,[a] Hongan Zhao,[a] Jianli Zhang,[a] Qinghua Liang,[b] Yining Wang,[a] Bailing Guo,[a] Raksha Dangol,[b] Yun Zheng,[b] Qingyu Yan,[b*] and Junwu Zhu[a*]

---

a. *Key Laboratory for Soft Chemistry and Functional Materials (Nanjing University of Science and Technology), Ministry of Education, Nanjing 210094, China.*
b. *School of Material Science and Engineering, Nanyang Technological University, Singapore 639798, Singapore.*
* *Corresponding authors:*
Junwu Zhu, E-mail: zhujw@njust.edu.cn
Qingyu Yan, E-mail: alexyan@ntu.edu.sg

Details about in-situ XRD measurement

The in-situ XRD measurement was conducted by using an in-situ battery. This configuration possesses a beryllium window that lets X-ray go through and reach the electrode while isolating the internal part of the ion battery from air. This design makes it possible to observe the phase change of the electrode by XRD during the charge/discharge process. The in-situ battery was assembled in an argon-filled glove box ($H_2O \leq 0.1$ ppm, $O_2 \leq 0.1$ ppm), using the same kind of separator, electrolyte and testing electrode in larger scale as that of 2032 coin-type battery. The related description can be found in the experimental part. The in-situ battery was installed on the XRD machine during the whole in-situ XRD test. After getting the initial phase of the electrode, galvanostatic charge-discharge process started under a current density of 0.2 A g^{-1} (from OC voltage discharging to 0.01 V then recharging to 3 V). The XRD patterns were collected at a speed of 7 min per cycle (from 10 to 80°) without any rest of the battery.

Method for particle size caculation

The average particle sizes were calculated by arithmetic mean value of hundreds of measured particle sizes. These particle sizes were measured from SEM images by software for particle size distribution analysis. The standard deviations of particle size for routine FeS_2 and F-FeS_2 are 51.7 and 17.7 nm, respectively.

Fig. S1 Digital photo of foam-like Fe_2O_3 precursor.

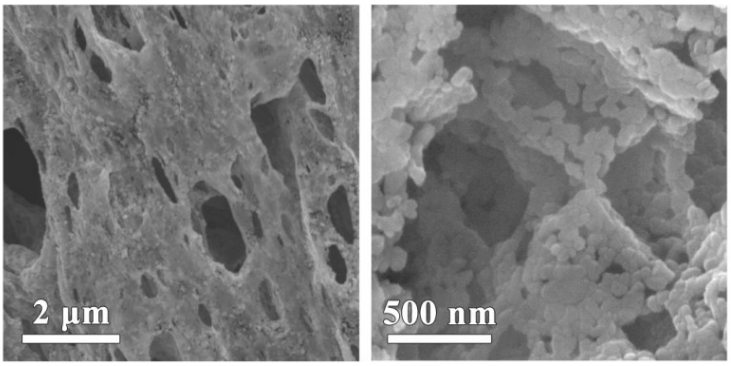

Fig. S2 SEM images of F-FeS_2 in different scales.

Sample	Mass (mg)	Fe mass by ICP (mg)	Fe ratio of FeS_2 by ICP (%)
F-FeS_2	50.9	23.6	46.4
FeS_2	50.6	23.4	46.2

Table S1 Inductively couples plasma determined elemental constituents measured in F-FeS_2 and routine FeS_2 samples.

The Table S1 shows the ICP-AES results of F-FeS_2 and FeS_2. It is noted that the Fe contents in all samples are very close to 46.7%, which matches well with that in FeS_2, suggesting the high purity of FeS_2.

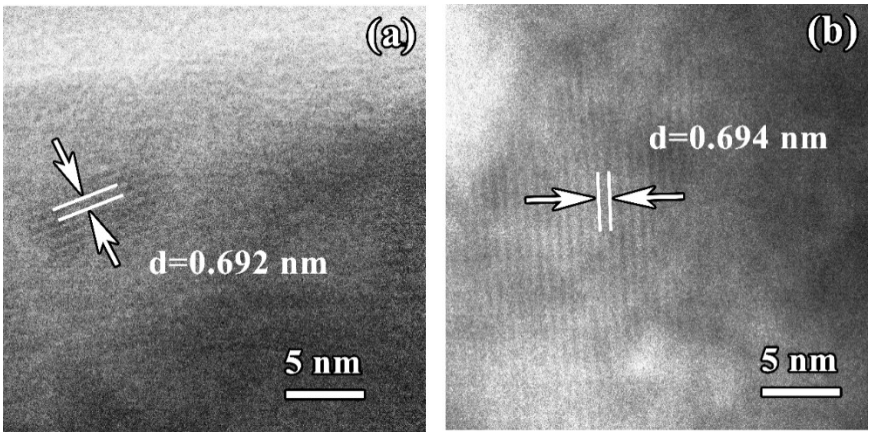

Fig. S3 The ex-situ HRTEM images of electrodes correspond to fixed CV stages. (a) Discharging to 1.07 V in the first cycle. (b) Discharging to 0.01 V and then recharging to 1.32 V in the first cycle.

After measuring the d-space of the strips, both lattice plane could be attributed to the (110) plane of $NaFeS_2$, proving the intercalation mechanism.

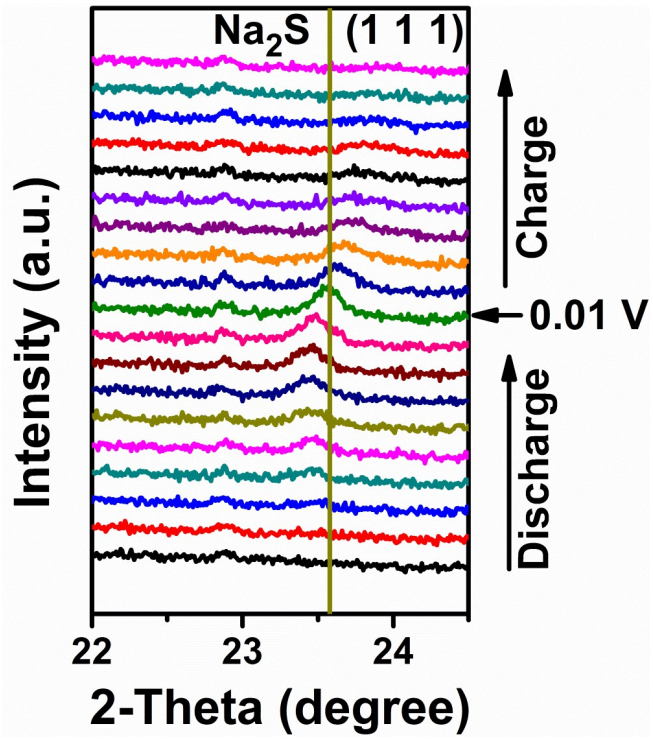

Fig. S4 Magnified in-situ XRD patterns of F-FeS_2 for SIB (focusing on Na_2S produced cycles).

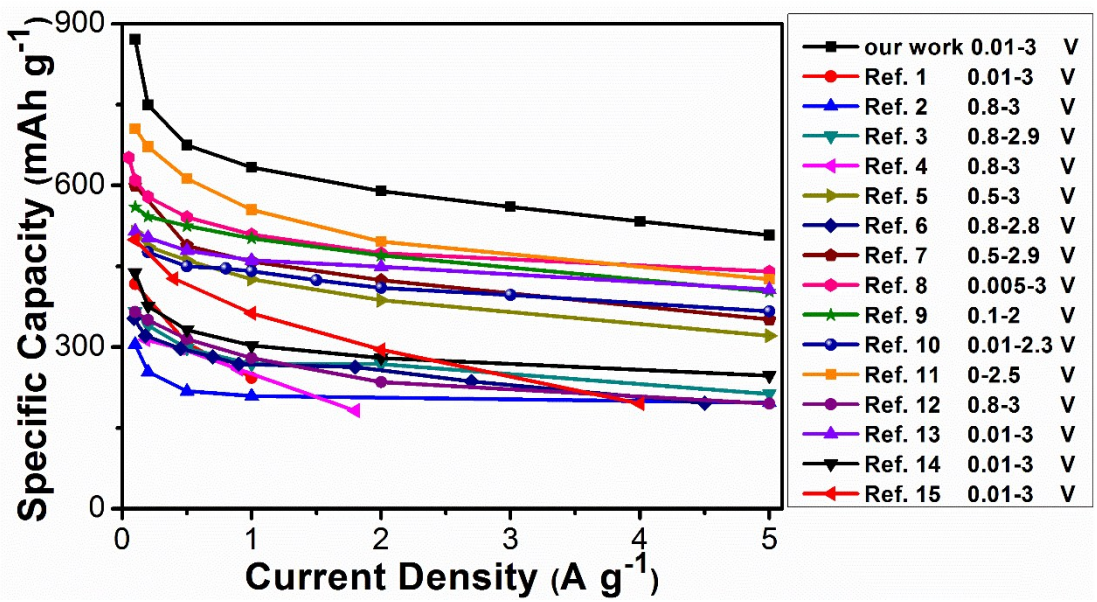

Fig. S5 Rate performance of ferric sulfides based SIBs compared with previous reports.[1-15]

The volumetric energy density of our F-FeS_2 is calculated to be 178 Wh L^{-1}.

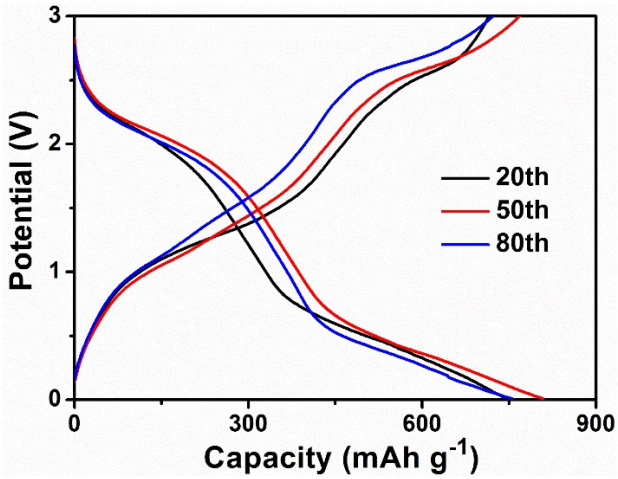

Fig. S6 The 20th, 50th and 80th GCD profiles at 0.2 A g^{-1} of F-FeS_2 for SIBs.

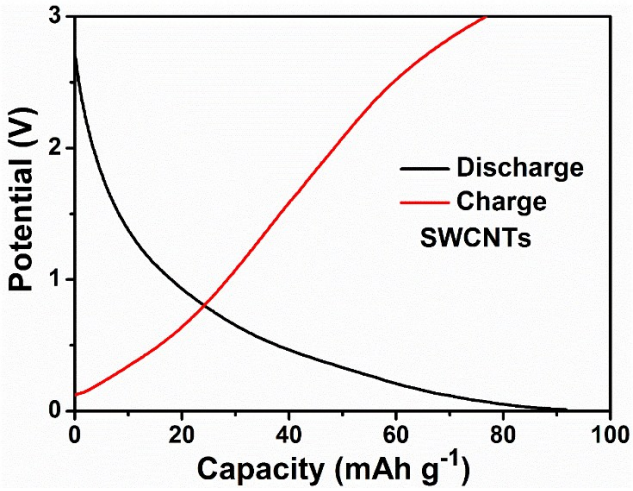

Fig. S7 The 5th GCD curves of SWCNTs at 0.1 A g^{-1} for NIBs.

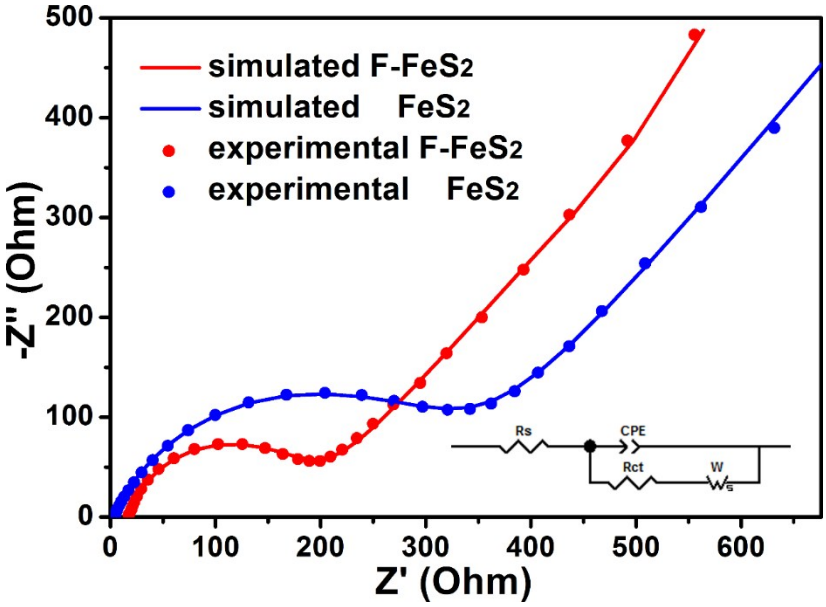

Fig. S8 The equivalent circuit and fitting lines of EIS data in Fig. 4c.

Sample	Rs (Ω)	Rct (Ω)	W-R	W-T	W-P
F-FeS_2	17.39	174.4	1905	3.516	0.55487
FeS_2	3.34	342	3667	4.61	0.57522

Table S2 Calculated resistance and Warburg coefficients based on the equivalent circuit in Fig. S8.

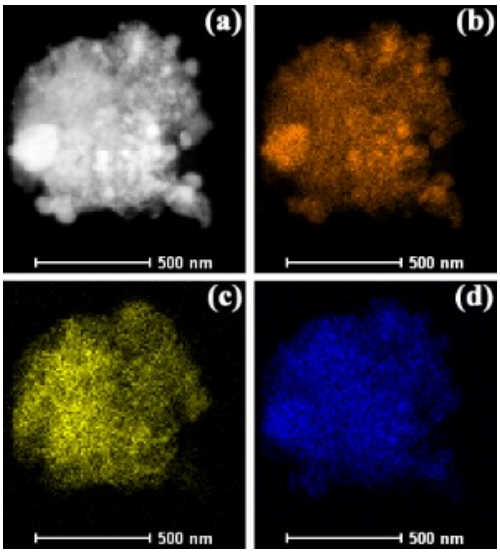

Fig.S9 EDX elemental mapping of (b) Na (c) S and (d) Fe in (a) F-FeS_2 particle discharged to 0.01 V after three discharge/charge cycles. The disappearance of S element around edge areas may be attributed to the anionic groups' dissolution in the ester-based electrolyte.

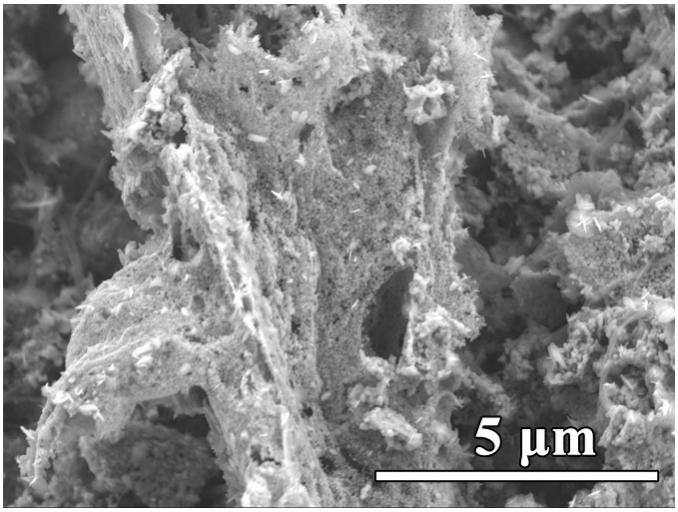

Fig. S10 SEM image of F-FeS_2 discharge/charge for three times.

Reference

1. A. Douglas, R. Carter, L. Oakes, K. Share, A. P. Cohn and C. L. Pint, *ACS Nano*, 2015, **9**, 11156-11165.
2. Z. Hu, Z. Zhu, F. Cheng, K. Zhang, J. Wang, C. Chen and J. Chen, *Energy Environ. Sci.*, 2015, **8**, 1309-1316.
3. K. Zhang, M. Park, L. Zhou, G. H. Lee, J. Shin, Z. Hu, S. L. Chou, J. Chen and Y. M. Kang, *Angew. Chem. Int. Edit.*, 2016, **55**, 12822-12826.
4. W. Chen, S. Qi, M. Yu, X. Feng, S. Cui, J. Zhang and L. Mi, *Electrochim. Acta*, 2017, **230**, 1-9.
5. K. Chen, W. Zhang, L. Xue, W. Chen, X. Xiang, M. Wan and Y. Huang, *ACS Appl. Mater. Inter.*, 2017, **9**, 1536-1541.
6. W. Chen, S. Qi, L. Guan, C. Liu, S. Cui, C. Shen and L. Mi, *J. Mater. Chem. A*, 2017, **5**, 5332-5341.
7. W. Zhao, C. Guo and C. M. Li, *J. Mater. Chem. A*, 2017, **5**, 19195-19202.
8. L. Li, S. Peng, N. Bucher, H.-Y. Chen, N. Shen, A. Nagasubramanian, E. Eldho, S. Hartung, S. Ramakrishna and M. Srinivasan, *Nano Energy*, 2017, **37**, 81-89.
9. Z. Liu, T. Lu, T. Song, X.-Y. Yu, X. W. Lou and U. Paik, *Energy Environ. Sci.*, 2017, **10**, 1576-1580.
10. Y. Xiao, J.-Y. Hwang, I. Belharouak and Y.-K. Sun, *ACS Energy Letters*, 2017, **2**, 364-372.
11. Q. Wang, C. Guo, Y. Zhu, J. He and H. Wang, *Nano-Micro Letters*, 2017, **10**, 30.
12. Z. Lu, N. Wang, Y. Zhang, P. Xue, M. Guo, B. Tang, Z. Bai and S. Dou, *Electrochim. Acta*, 2018, **260**, 755-761.
13. B. H. Hou, Y. Y. Wang, J. Z. Guo, Q. L. Ning, X. T. Xi, W. L. Pang, A. M. Cao, X. Wang, J. P. Zhang and X. L. Wu, *Nanoscale*, 2018, **10**, 9218-9225.
14. D. Li, Y. Sun, S. Chen, J. Yao, Y. Zhang, Y. Xia and D. Yang, *ACS Appl. Mater. Inter.*, 2018, **10**, 17175-17182.
15. F. Bu, P. Xiao, J. Chen, M. F. Aly Aboud, I. Shakir and Y. Xu, *J. Mater. Chem. A*, 2018, **6**, 6414-6421.